Interwire coupling for In(4 × 1)/Si(111) probed by surface transport

F. Edler,[1] I. Miccoli,[1] S. Demuth,[1] H. Pfnür,[1,2] S. Wippermann,[3] A. Lücke,[4] W. G. Schmidt,[4] and C. Tegenkamp[1,2,*]

[1]*Institut für Festkörperphysik, Leibniz Universität Hannover, Appelstraße 2, 30167 Hannover, Germany*

[2]*Laboratorium für Nano- und Quantenengineering (LNQE), Leibniz Universität Hannover, Schneiderberg 39, 30167 Hannover, Germany*

[3]*Grenzflächenchemie und Oberflächentechnik, Max-Planck-Institut für Eisenforschung GmbH, Max-Planck-Straße 1, 40237 Düsseldorf, Germany*

[4]*Lehrstuhl für Theoretische Physik, Universität Paderborn, 33098 Paderborn, Germany*

(Received 29 May 2015; revised manuscript received 10 July 2015; published 25 August 2015)

The In/Si(111) system reveals an anisotropy in the electrical conductivity and is a prototype system for atomic wires on surfaces. We use this system to study and tune the interwire interaction by adsorption of oxygen. Through rotational square four-tip transport measurements, both the parallel ($\sigma_{||}$) and perpendicular ($\sigma_{\perp}$) components are measured separately. The analysis of the I(V) curves reveals that $\sigma_{\perp}$ is also affected by adsorption of oxygen, showing clearly an effective interwire coupling, in agreement with density-functional-theory-based calculations of the transmittance. In addition to these surface-state mediated transport channels, we confirm the existence of conducting parasitic space-charge layer channels and address the importance of substrate steps by performing the transport measurements of In phases grown on Si(111) mesa structures.

DOI: 10.1103/PhysRevB.92.085426 PACS number(s): 68.37.−d, 73.20.−r, 72.15.−v, 72.10.Fk

I. INTRODUCTION

The In/Si(111) system is, to date, probably the best studied atomic wire ensemble and a prototype system for metal-insulator transitions (MITs) in quasi-one-dimensional adsorbate structures. This system has been comprehensively characterized by various experimental techniques as well as *ab initio* theory, as recently reviewed in Refs. [1,2].

Besides this MIT [3], the system reveals high anisotropy in conductivity even at room temperature. By means of a scanning tunneling microscopy (STM)-based four-tip transport technique, the conductivity components both along ($\sigma_{||}$) and perpendicular to ($\sigma_{\perp}$) the direction of the wires were measured [4,5], revealing anisotropy values as high as $\sigma_{||}/\sigma_{\perp} \approx 60$ [4]. This anisotropy agrees remarkably well with the effective mass tensor obtained from the analysis of the surface states at the Fermi energy E_F [2]. However, this agreement may be partially fortuitous, since experimentally there is evidence for a space-charge layer contribution to the conductivity (σ_{SCL}), which was not accounted for in the calculations.

In order to address this puzzling finding in greater detail, this subject was revisited recently [6]. Depending on details of the preparation, it was shown that indeed the $\sigma_{\perp}$ component correlates with the flash-annealing temperature used for cleaning and preparation of the Si(111) surfaces. Apparently, high-temperature flash annealing in vacuum leads to the formation of a *p*-type epilayer. The associated flat-band condition in this area gives rise to an isotropic σ_{SCL} background in addition to contributions from surface states. Moreover, the transport measurements by Uetake *et al.* suggest that the residual conductance channel across the wires is entirely caused by σ_{SCL} [6].

The MIT in the In/Si(111) system is the result of a balanced intra- and interwire coupling [7–10]. For instance, the metal-insulator transition is correlated with the appearance of the ×8 diffraction spots, i.e., with order between adjacent wires. This underlines a notable interwire coupling, which should also be reflected by the conductivity components measured at room temperature. Moreover, its transition temperature can be tuned or even quenched by various adsorbates [11,12]. In this study, we restrict ourselves to the adsorption of oxygen, which chemisorbs dissociatively at room temperature on In/Si(111) [13], in agreement with theory [14]. Interestingly, oxygen increases T_c, while many other adsorbates show the opposite behavior [15,16]. Moreover, it was shown that single oxygen defects also induce a structural phase transition in the adjacent defect-free In chain [17]. How the impurities feed back in detail to the phase transition is unknown and under current debate [13,18,19].

A recent STM and density-functional theory (DFT) study revealed that atomic oxygen adsorbs on threefold coordinated intrachain sites, either above or below one of the two zigzag chains or between them [14,20]. From angle-resolved photoemission spectroscopy (ARPES), it is known that the band fillings increase by around 7% at 10 L O_2, i.e., oxygen injects electrons [13]. For low-oxygen coverages, the band-filling factors and band structure are almost unchanged. Therefore, the change of the conductivity measured at room temperature is mainly related to the electronic mobility, i.e., to the scattering times. First transport measurements under the influence of oxygen revealed that $\sigma_{\perp}$ is not affected [21]. As we will show in this study, this contrasts with our findings.

Transport measurements on a two-dimensional (2D) ensemble structure, although performed with local probe techniques, inevitably probe a quasi-infinite area, i.e., in addition to near-surface modifications and transport anisotropy induced by the coupling of wires, the Si substrate steps are also important and influence the transport findings. The way to grow single-domain In phases is to use Si(111) samples with a slight miscut towards the $[\bar{1}\bar{1}2]$ direction. Typically, the miscut angles vary between 1°–4° [21–24], i.e., the surface exhibits between 5 to 20 steps per 10 μm. From potentiometry and transport measurements, it is known that monatomic steps significantly increase the resistance [25–27], and thus the

*tegenkamp@fkp.uni-hannover.de

vicinality of the Si(111) surface should have an effect on the In/Si(111) anisotropy.

In order to shed light on these different contributions, we performed surface-sensitive transport measurements on spatially restricted anisotropic 2D phases. In contrast to previous experiments, we found that the conductivity perpendicular to the wires $\sigma_\perp$ is clearly affected. The modification of the interwire coupling due to oxygen adsorption is supported by DFT calculations showing indeed a crosstalk between defective and perfect adjacent In wires.

II. EXPERIMENT AND COMPUTATIONAL METHODS

Samples of Si(111) substrate with a nominal miscut of 1° towards the $[\bar{1}\bar{1}2]$ direction were used (n type, $\rho = 500$–$800\ \Omega$ cm). In order to avoid contributions from the space-charge layer in our transport experiments, the samples were first cleaned through a vigorous chemical treatment including standard RCA-1 etching [28] in air and subsequent flash annealing under UHV conditions to 1000 °C at most, while maintaining a pressure below 7×10^{-10} mbar. Single domain In(4×1) structures were grown at 400 °C. The overall quality of both the substrate and the In phase as well as the orientation were controlled by spot-profile-analysis low-energy electron diffraction [SPA-LEED; cf. Fig. 1(a)]. The Si(111) samples also hosted circular mesas of different sizes (diameter 15–40 μm), which were prepared *ex situ* by optical lithography on one-half of the sample (etching depth 500 nm). As we will show below, these spatially restricted (and vertically lifted) structures reveal different anisotropies and space-charge layer contributions. Four-point-probe (4PP) transport experiments were performed at room temperature by means of a four-tip STM system (Omicron Nanoprobe) using NaOH-etched W tips. All measurements on confined areas shown below were performed on the smallest mesas. Since typical probe spacings on the quasi-infinite 2D phases were around 15 μm, they are comparable with measurements on the mesas. The conductivity values as well as the anisotropy were determined by the so-called rotational square method, described in detail in Ref. [5]. Besides LEED, the clean In(4×1) phase has also been characterized by temperature-dependent transport measurements on the quasi-infinite areas. The metal-insulator transition found at 120 K (not shown) is fully in line with former studies [3,16] and indicative of an electronically intact In phase. As we will show below, the avoidance of high annealing temperatures to first order only affects the defect density along the wires, and gives rise to comparably low $\sigma_{||}$ values. All oxygen-dose experiments were done via a leak valve using a background pressure of 3×10^{-7} mbar.

In order to rationalize and interpret the experimental findings, DFT calculations within the local-density approximation (LDA) were performed utilizing the structural models recently obtained for oxygen adsorption on the In(4×1) phase [20]. The subtle energetics of the In/Si(111) systems has been shown to be very sensitive with respect to the details of the exchange-correlation functional used [10,29] and even with respect to relativistic and spin-orbit coupling effects [30]. However, partially due to a fortuitous error cancellation, DFT-LDA provides meaningful total energies, atomic structures, as well as vibrational and optical properties for In/Si(111) [9,31].

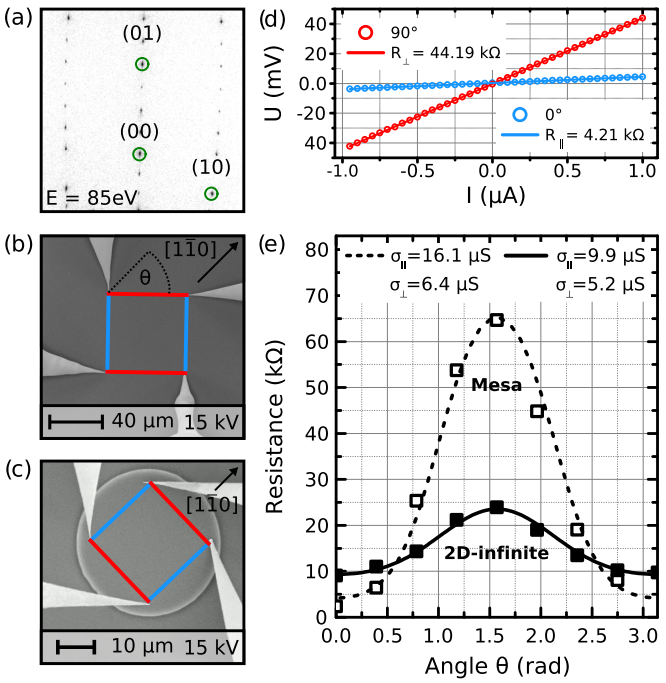

FIG. 1. (Color online) (a) LEED image demonstrating the growth of a long-range ordered single-domain structure. (b) Scanning electron microscopy (SEM) image of four W tips placed in a square configuration on In(4×1) on Si(111). (c) The four tips placed on a circular In/Si(111)-mesa structure (40 μm diameter). (d) I(V) curves obtained for the two distinct configurations (current along the red and blue lines, respectively). The different slopes reflect the anisotropy of the conductivity. (e) The resistance measured in a square 4PP geometry at room temperature as a function of the angle (zero along the direction of the In wires). The resistance anisotropy on a spatially constricted 2D phase (15 μm) is significantly higher than for the quasi-infinite 2D case. 0° refers to a parallel orientation of the current probes. Both measurements on constricted and free areas were done with the same probe spacings (15 μm) on the same sample.

Given the large unit cells that need to be considered here, the DFT-LDA approach used earlier [9] is a very meaningful compromise between accuracy and numerical expense for the present calculations.

In particular, quantum transport calculations were performed using the scattering approach proposed by Choi *et al.* [32] and Smogunov *et al.* [33] as implemented in the PWCOND module [34] of the QUANTUM-ESPRESSO package [35]. This allows one to determine the coherent transmission coefficients $\mathfrak{T}$ through the oxygen-contaminated indium wires. The transport-system setup is depicted below in Sec. III C for the two relevant transport directions along and perpendicular to the wires. Such a system setup consists of two parts: (i) the ideal contacts which are followed up periodically to semi-infinite contacts and (ii) the enclosed scatter region which contains the impurities. In order to make the parameter-free solution of the scattering problem feasible for the large adsystems, the silicon substrate in the super cell is modeled with one double layer saturated with hydrogen. This affects the most transport-relevant In bands only marginally compared to a supercell with three double layers of Si substrate and leads to a numerical error bar of the calculated transmittance $\mathfrak{T}$ of less

than 10%. The Brillouin zone of the 4 × 1 unit cell is sampled with a 16 (intrachain) × 4 (interchain) × 1 Monkhorst-Pack mesh of special **k** points [36]. Equivalent **k**-point meshes have been used for larger unit cells. Other technical parameters were chosen as in our previous In nanowire studies [20,30].

III. RESULTS AND DISCUSSION

A. Finite-size effects in anisotropic 2D systems

The successful growth of single-domain In wires with (4 × 1) symmetry on Si(111) samples with 1° miscut is obvious from the LEED picture shown in Fig. 1(a). The In wires are running along the [1$\bar{1}$0] direction. For transport measurements, the W tips have been sequentially approached in a feedback-controlled manner, thus avoiding irreversible damages to probes and surface [Fig. 1(b)]. The resistance is deduced from a linear fit of the IV curves, as shown exemplarily in Fig. 1(d) for two configurations, where the connecting lines between the current probes are either parallel or perpendicular to the direction of the wires. As is obvious, the resistances reveal an asymmetry which reflects the anisotropy of the conductivity. In case of a quasi-infinite 2D layer, measured with probes in a square 4PP geometry, the resistance along (perpendicular to) the direction of the atomic wires is given by $R_{||(\perp)} = (2\pi\sqrt{\sigma_{||}\sigma_{\perp}})^{-1}\ln(1+\sigma_{||(\perp)}/\sigma_{\perp(||)})$, where $\sigma_{||}$ and $\sigma_{\perp}$ denote the conductivity components along and parallel to the [1$\bar{1}$0]direction, respectively.

A more reliable method to determine both the anisotropy and, simultaneously, the orientation of the wires is the so-called rotational square micro-4PP method where the squared 4P assembly is rotated with respect to the In(4 × 1). Details are elaborated in Refs. [4,5]. According to this method, the resistances are measured for various angles and are plotted in Fig. 1(e) for the quasi-infinite 2D phase. The solid line is a fit to the data and yields for the case shown in Fig. 1(e) conductivity values of $\sigma_{||} \approx 10\ \mu$S/□ and $\sigma_{\perp} \approx 5\ \mu$S/□. We admit that the anisotropy measured in this case ($\sigma_{||}/\sigma_{\perp} = 2$) is significantly lower than the values reported in Ref. [4], but it is close to those reported in a recent study [6]. We will see in the following that phase inhomogeneities, e.g., induced by atomic steps, reveal much higher resistance anisotropies.

Any structural defects, e.g., lateral constrictions or atomic steps, significantly increase the resistance (R) anisotropy. In order to demonstrate this, we also measured the R anisotropy for In wire ensembles on finite Si(111)-mesa structures [cf. Fig. 1(c)]. Compared to the quasi-infinite case, the $R(\Theta)$ curve in Fig. 1(e) clearly reveals a distinct increase by almost one order of magnitude. The fit to the data (dashed line) reveals conductivities of $\sigma_{||} \approx 16\ \mu$S/□ and $\sigma_{\perp} \approx 6\ \mu$S/□, i.e., the anisotropy measured on the Si(111) mesa is only marginally increased with respect to the quasi-infinite case. Details about the fit function for laterally confined phases can be found in Ref. [5]. Please note that the difference between resistance anisotropies is by far not reflected by the conductivity ratios, nicely demonstrating that boundaries indeed play a crucial role. Both transport measurements were performed on the same sample (at different sites), and thus the conductivity components measured on these phases should be the same. This is almost the case, as seen for the $\sigma_{\perp}$ values, showing

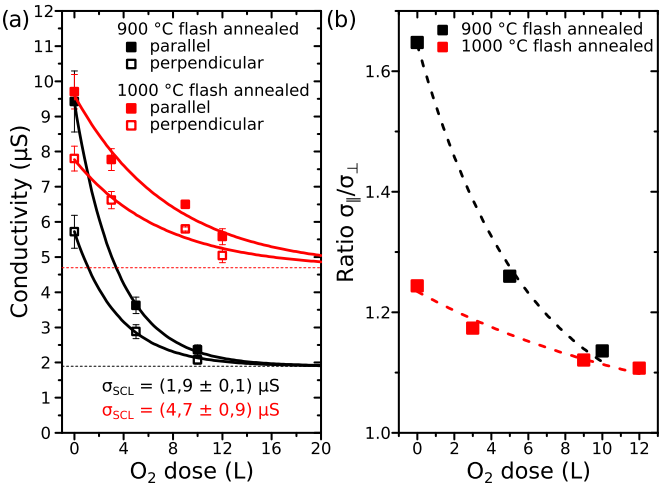

FIG. 2. (Color online) Transport measurements performed on quasi-infinite 2D In(4 × 1) phase. (a) $\sigma_{||}$ and $\sigma_{\perp}$ as a function of the O_2 dose and flash-annealing temperature. The isotropic background refers to a contribution of the space-charge layer σ_{SCL}. (b) Decrease of the anisotropy $\sigma_{||}/\sigma_{\perp}$ as a function of the O_2 dose.

that the average step density along the [$\bar{1}\bar{1}$2] direction has not changed significantly. The slight increase of the conductivity anisotropy is probably accounted for by an increased $\sigma_{||}$ value for In wires grown on Si-mesa templates. The finite size of such a template may favor step straightening and thus trigger growth of extended In wires with an increased electronic mean free path. An influence of stress for tuning the step morphology is known from other investigations [37].

B. Adsorption of molecular oxygen

Figure 2(a) shows the different conductivity components measured on quasi-infinite 2D In phases grown on differently prepared Si surfaces as a function of oxygen dose. Before the effect of oxygen adsorption is discussed, we first draw attention to the effect of the sample preparation by thermal annealing at 900 °C and 1000 °C prior to adsorption of In. Higher flash temperatures were not considered, since otherwise the mesa structures became irreversibly damaged. As is obvious, the absolute conductivities and anisotropies are influenced by the pretreatment of the Si sample. While annealing at 900 °C yields larger anisotropy ratios [cf. Fig. 2(b)], higher annealing temperatures primarily increase $\sigma_{\perp}$. These effects come along with the gradual increase of an isotropic background, which has been interpreted recently by the formation of a space-charge layer (see below) [6]. This underlines that the near-surface area is severely modified by the high-temperature annealing procedures, which affect the transport properties of the In wires. Generally, higher annealing temperatures tend to result in cleaner and long-range ordered surfaces. Therefore, increased $\sigma_{||}$ values are expected as a function of increased annealing temperature, which is only to some extent visible in the case of the quasi-infinite 2D sample [cf. Fig. 2(a)]. Apparently, the miscut angle of the sample, i.e., the step-step interaction, is a further critical parameter, which not only influences the growth of single domains but also determines the average lengths of the wires. Similar trends were found

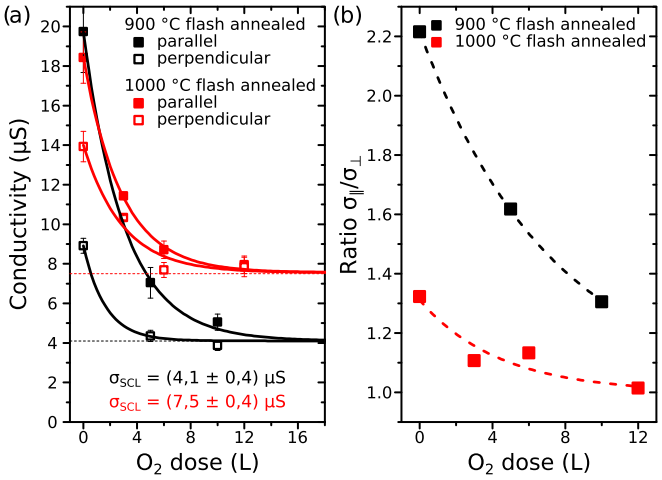

FIG. 3. (Color online) The same transport measurements as in Fig. 2, but performed on a Si(111)-mesa structure as shown in Fig. 1(c). (a) $\sigma_{||}$ and $\sigma_{\perp}$ as a function of the O_2 dose and flash-annealing temperature. The isotropic background refers to a contribution of the space-charge layer σ_{SCL}. (b) Decrease of the anisotropy $\sigma_{||}/\sigma_{\perp}$ as a function of the O_2 dose.

on Si-mesa structures, which will be discussed in context with Fig. 3.

Upon adsorption of oxygen, both $\sigma_{||}$ and $\sigma_{\perp}$ for the quasi-infinite case decrease with increasing dose (D) of molecular oxygen. Our results show unambiguously that both the intra- and interwire couplings are affected by adsorption. In former experiments, where molecular oxygen and the residual gas were used in a long-term experiment, a change of the $\sigma_{\perp}$ component was not reported [6,21]. Furthermore, both components saturate at a finite value, i.e., the surface-state mediated transport channels are superimposed by an isotropic background. This background is robust against further adsorption of oxygen and thus reminiscent of a buried transport channel, e.g., of a space-charge layer, as already pointed out by Uetake *et al.* [6].

Quantitatively, the conductivities measured as a function of the O_2 dose (D) can be described by $\sigma_{||,(\perp)}(D) = \sigma_{||,(\perp)}(0)\, e^{-D/D_{0,||(0,\perp)}} + \sigma_{SCL}$. The space-charge layer contributions found for annealing the Si substrate to 900 °C and 1000 °C are 1.9 μS/□ and 4.7 μS/□, respectively, and are in agreement with the trend reported by Uetake *et al.* [6]. The formation of the space-charge layer is caused by temperature-induced p-type doping at the vacuum interface, although n-type wafers were used [38,39]. For the quasi-infinite 2D case, the decay along the wires for 900 °C is $D_{0,||} = 3.4\ \mathrm{L}^{-1}$ and is in agreement with a previous study [21]. For this particular case, the decay of the conductivity along the interwire direction is slightly weaker ($D_{0,\perp} = 3.6\ \mathrm{L}^{-1}$), but generally similar, showing that oxygen affects both transport channels in the same way. Within our analysis and by following the arguments given by Okino *et al.* [21], an influence of the oxygen atoms on the space-charge layer has been neglected, as both spectroscopic investigations as well as calculations revealed rather a modification of the surface states upon adsorption [13,40].

The oxygen-adsorption experiments were also performed and investigated for the In phase on Si(111) mesas. The results obtained for the conductivity and anisotropy values are summarized in Fig. 3. Again, the highest anisotropies are obtained for flash-annealing temperatures not exceeding 900 °C. Upon adsorption, both components decrease with increasing oxygen coverage, supporting our conclusions above. Most interestingly, the σ_{SCL} background is increased on the mesa structure by a factor of 1.9 ± 0.2 compared to the data presented in Fig. 2. Assuming that the mesa structure with a nominal height of 500 nm reveals entirely p-type character, the thickness of the p-type region within the quasi-infinite regime is around 550 nm, which is in reasonable agreement with estimations given in Ref. [6]. As obvious from Fig. 3, in the saturated regime the electronic transport occurs via the space-charge layer, i.e., in the case of the Si-mesa structure, the currents are not necessarily restricted any longer to the mesa itself, implying that possibly different corrections factors are needed. Therefore, in the case of the anisotropic transport regime, different correction factors are probably mandatory, e.g., for the finite 2D scenario, assumed here for a clean surface which is justified as long as the surface-state contribution dominates the transport signal, and the 2D infinite scenario (saturated regime). However, after dosage of 15 L, the R ratio is unity, i.e., the conductivities measured with our tip geometry for the alleged confined regime and 2D infinite case reveal the same conductivities [5]. Note that such considerations are not necessary for the quasi-infinite 2D case discussed in the context of Fig. 2, i.e., our general conclusions will not be affected by the space-charge layer implications in the case of the Si-mesa structure. For further details, see Ref. [5].

So far, our experiments have confirmed the presence of a space-charge layer contribution and that its magnitude depends on details of the pretreatment of the Si sample. Second, we have also shown that $\sigma_{\perp}$ is affected by the adsorption of oxygen; in other words, the In-induced surface states now also contribute to the transport channel in the direction across the wires.

C. DFT calculations: LDOS and transmission functions

Here we will concentrate on the oxygen-induced effect on $\sigma_{\perp}$ and will start with a brief summary regarding the adsorption behavior found in previous studies. The oxygen-adsorption sites were determined by high-resolution STM and were confirmed by DFT calculations [20]. According to these studies, oxygen prefers to adsorb on top within a threefold coordinated position in one of the two zigzag In chains (so-called α-type defect) [14,20,40]. With a probability of around 30%, other adsorption sites were found, where the oxygen adsorbs at the Si/In interface (β defect) or between the two zigzag In chains (γ defect), respectively. The statistical analysis of STM images further revealed that a dose of 3 L at room temperature results in defect concentrations of 8×10^{12} cm^{-2} [20] (cf. with 4×10^{12} cm^{-2} in Ref. [21]). This corresponds to a defect concentration of around 4% with respect to the (4×1) unit cell. Recent ARPES measurements have shown that the overall electronic structure of the In surface bands is not drastically altered. The band-filling factors are increased by around 7% after dosing 10 L O_2 [13]. Qualitatively, this is in line with calculations that found an oxygen-induced local modification

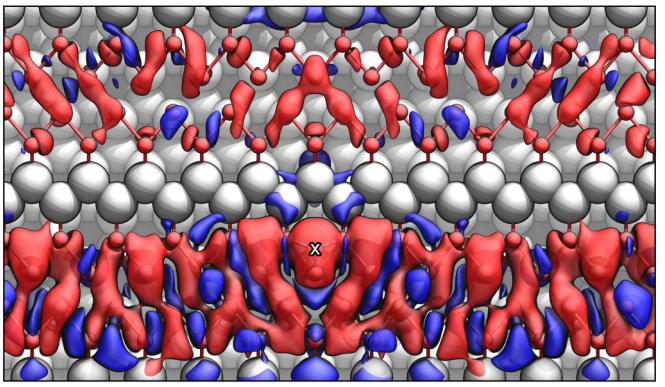

FIG. 4. (Color online) Difference of local density of states (LDOS) within a 8×12 unit cell integrated within an interval of ± 0.1 eV centered at E_F around an α-type oxygen α-type defect (marked by a cross) compared to ideal, defect-free wires. The increase (decrease) of the LDOS is colored in blue (red). The corresponding isovalues are set to 1×10^{-5} and -7.5×10^{-5}, respectively.

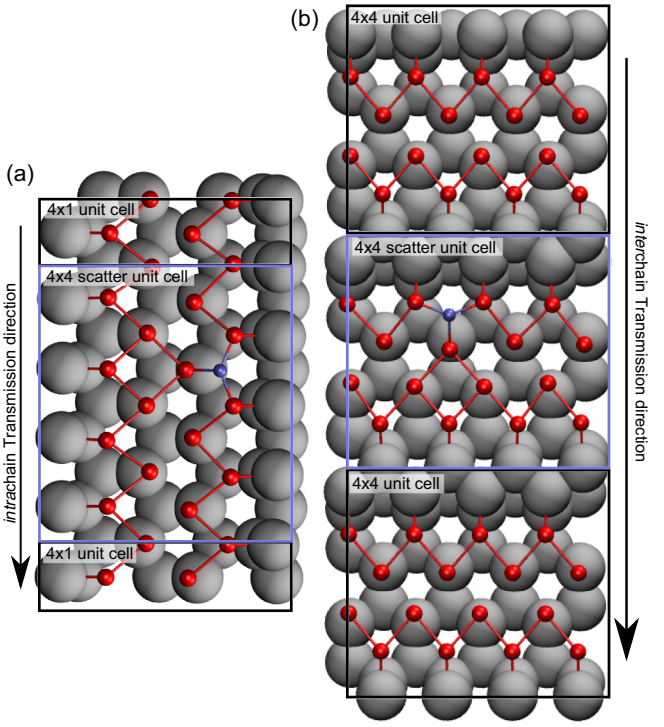

FIG. 5. (Color online) Schematic setup of the transport calculations for the (a) intrachain and (b) interchain direction. The (4×4) unit cell containing the O scatterer (purple frame) is sandwiched between ideal wire segments that model semi-infinite ideal contacts (black frame).

of the electron potential coupled with a reduction of the electronic transmission along the wires by around 50% for the α-type defects [40]. In particular, the lattice distortion upon adsorption overcompensates the weak doping, resulting in an overall reduction of conductance.

One may argue that the adsorption of oxygen in this study is severely influenced by the initial defect density of the pristine In phase. Compared to the transport experiments performed on high-temperature annealed and on higher-miscut Si(111) surfaces [4], the conductivity values in our case along the wires are lower by one order of magnitude, i.e., relying on defect-induced transmission coefficients of 50% [40], the defect concentration along the wires must be approximately four times higher. As deduced from STM images of the pristine In phase, the (intrinsic) defect concentration is of the order of 1×10^{12} cm^{-2} [21]. This means that the intrinsic defect concentration in our case is around 5×10^{12} cm^{-2}, which is equivalent to a dosage of 1–2 L of O_2. Therefore, as the gradual decrease of conductance along both directions is seen even for higher dosages, our findings are not limited by the structural imperfections, but are more likely due to the modification of the In(4×1) itself.

Density-functional calculations of the local density of states (LDOS) at E_F show that oxygen atoms severely affect the electronic structure of the In wire they adsorb on; see also Ref. [20]. Interestingly, it is found that the LDOS is perturbed not only in the immediate vicinity of the adatom, but ranges several lattice constants along the wire direction. In addition to this, there is also a cross talk with the neighboring In wire, which should affect the transport in the direction across the wires. Figure 4 shows the difference of the LDOS (integrated over ± 0.1 eV around E_F) with respect to the perfect (4×1) phase. As is obvious, the adsorption of oxygen changes the density of states (DOS) at E_F also on the neighboring In chain and the tiny fractions of a local increase in the DOS are overcompensated by areas with a reduced DOS (marked in red).

In order to quantify the influence on transport of the most common α-type oxygen defect onto the quantum transport properties of the indium nanowires, we apply a coherent-transport model along and perpendicular to the indium wires. Therefore, we use a (4×4) surface unit cell that contains a single oxygen adatom which is roughly comparable to the dosage 15 L of O_2 in the experiment. This unit cell is sandwiched between ideal contact elements, as depicted in Fig. 5.

For the configuration shown in Fig. 5(a), the transmittance decreases to around $\mathfrak{T}_{||}(15\text{ L})/\mathfrak{T}_{||}(0\text{ L}) \approx 0.65$ in the parallel (=intrachain) direction. This agrees quantitatively with previous transport calculations based on a Green's-function formalism [40] where it has been shown that oxygen strongly affects the conductivity along the wires mainly due to the combination of two effects: On the one hand, O adatoms form a potential well that effectively scatters the electrons, thus reducing the transmittance. On the other hand, oxygen adsorption leads to geometric deformations of the In nanowires that reduce its conductance. Relying on the configuration shown in Fig. 5(b), the transmission across the direction of the wires also has been investigated. The calculation reveals, for one oxygen defect per (4×4) unit cell, a ratio of $\mathfrak{T}_{\perp}(15\text{ L})/\mathfrak{T}_{\perp}(0\text{ L}) \approx 0.45$, i.e., the coherent transport perpendicular to the wires is even slightly more affected than the parallel transport. The values calculated here are in good agreement with the measurements, considering the isotropic background due to the space-charge layer that is not included in the calculations.

Moreover, it should be considered that the realization of contacts by semi-infinite perfect In units underestimates the

effect of the oxygen defect within the (4×4) unit cell, i.e., the effective defect concentration in the calculation is lower. In order to investigate the effect of higher defect concentrations and mimic to some extent the experimental situation of a diffusive transport regime, calculations considering two subsequent scattering units were also performed. Interestingly, the additional transmittance decrease along the wires is stronger than in the interwire direction, which is in qualitative agreement with the present experimental findings (cf. with Fig. 2). Relying on the fact that the conductivity along the wire is higher compared to the $[\bar{1}\bar{1}2]$ direction, as correctly modeled within an effective mass tensor calculation [2], the trend seen for the direction-dependent transmittance factors in this study would finally result in an isotropic electronic transport in accordance with our experiments.

IV. SUMMARY AND CONCLUSION

In this study, we analyzed the conductivity anisotropy for In/Si(111) on infinite and spatially restricted 2D phases. The parasitic background due to the formation of a space-charge layer can be minimized by using moderate flash temperatures. However, these moderate flash temperatures come along with comparably low $\sigma_{||}$ values, giving rise to low anisotropies, at least for Si(111) samples with a low step density along the $[\bar{1}\bar{1}2]$ direction. The contributions of the surface states are gradually reduced by adsorption of molecular oxygen at room temperature. Thereby, the decrease of $\sigma_{\perp}$ with increasing oxygen dose underlines the interwire coupling in this alleged quasi-1D system and is quantified by quantum-conductance calculations. Nonetheless, comparing the present calculations to the measured findings, one should consider further that the effect of realistic contacts, i.e., their scattering behavior, as well as thermal dissipative scattering due to phonons at finite temperature are not included in the simulations. Despite these limitations, the present coherent-transport calculations describe surprisingly well the oxygen-induced conductance modifications observed experimentally. Most importantly, they clearly show that oxygen defects affect the conductance perpendicular to the In wire direction.

ACKNOWLEDGMENTS

Financial support by the Deutsche Forschungsgemeinschaft through FOR1700 as well as grants of computer time provided by the HLRS Stuttgart and the Paderborn PC^2 are gratefully acknowledged.

[1] P. C. Snijders and H. Weitering, Rev. Mod. Phys. **82**, 307 (2010).
[2] W. G. Schmidt, S. Wippermann, S. Sanna, M. Babilon, N. J. Vollmers, and U. Gerstmann, Phys. Status Solidi B **249**, 343 (2012).
[3] T. Tanikawa, I. Matsuda, T. Kanagawa, and S. Hasegawa, Phys. Rev. Lett. **93**, 016801 (2004).
[4] T. Kanagawa, R. Hobara, I. Matsuda, T. Tanikawa, A. Natori, and S. Hasegawa, Phys. Rev. Lett. **91**, 036805 (2003).
[5] I. Miccoli, F. Edler, H. Pfnür, and C. Tegenkamp, J. Phys.: Condens. Matter **27**, 223201 (2015).
[6] T. Uetake, T. Hirahara, Y. Ueda, N. Nagamura, R. Hobara, and S. Hasegawa, Phys. Rev. B **86**, 035325 (2012).
[7] J. R. Ahn, J. H. Byun, H. Koh, E. Rotenberg, S. D. Kevan, and H. W. Yeom, Phys. Rev. Lett. **93**, 106401 (2004).
[8] K. Fleischer, S. Chandola, N. Esser, W. Richter, and J. F. McGilp, Phys. Rev. B **76**, 205406 (2007).
[9] S. Wippermann and W. G. Schmidt, Phys. Rev. Lett. **105**, 126102 (2010).
[10] Hyun-Jung Kim and Jun-Hyung Cho, Phys. Rev. Lett. **110**, 116801 (2013).
[11] S. V. Ryjkov, T. Nagao, V. G. Lifshits, and S. Hasegawa, Surf. Sci. **488**, 15 (2001).
[12] H. Morikawa, C. C. Hwang, and H. W. Yeom, Phys. Rev. B **81**, 075401 (2010).
[13] S. H. Uhm and H. W. Yeom, Phys. Rev. B **88**, 165419 (2013).
[14] H. Shim, H. Lim, Y. Kim, S. Kim, G. Lee, H.-K. Kim, C. Kim, and H. Kim, Phys. Rev. B **90**, 035420 (2014).
[15] Geunseop Lee, Sang-Yong Yu, Hyungjoon Shim, Woosang Lee, and Ja-Yong Koo, Phys. Rev. B **80**, 075411 (2009).
[16] T. Shibasaki, N. Nagamura, T. Hirahara, H. Okino, S. Yamazaki, W. Lee, H. Shim, R. Hobara, I. Matsuda, G. Lee, and S. Hasegawa, Phys. Rev. B **81**, 035314 (2010).
[17] S. Wippermann, H. W. Yeom *et al.* (unpublished).
[18] S. Wall, B. Krenzer, S. Wippermann, S. Sanna, F. Klasing, A. Hanisch-Blicharski, M. Kammler, W. G. Schmidt, M. Horn-von Hoegen, Phys. Rev. Lett. **109**, 186101 (2012).
[19] H. Shim, J. Yeo, G. Lee, and H. Kim, Phys. Rev. Lett. **111**, 149601 (2013).
[20] D. M. Oh, S. Wippermann, W. G. Schmidt, and H. W. Yeom, Phys. Rev. B **90**, 155432 (2014).
[21] H. Okino, I. Matsuda, R. Hobara, S. Hasegawa, Y. Kim, and G. Lee, Phys. Rev. B **76**, 195418 (2007).
[22] T. Abukawa, M. Sasaki, F. Hisamatsu, T. Goto, T. Kinoshita, A. Kakizaki, and S. Kono, Surf. Sci. **325**, 33 (1995).
[23] J. L. Stevens, M. S. Worthington, and I. S. T. Tsong, Phys. Rev. B **47**, 1453 (1993).
[24] K. Fleischer, S. Chandola, N. Esser, W. Richter, J. F. McGilp, W. G. Schmidt, S. Wang, W. Lu, and J. Bernholc, Appl. Surf. Sci. **234**, 302 (2004).
[25] I. Matsuda, M. Ueno, T. Hirahara, R. Hobara, H. Morikawa, C. Liu, and S. Hasegawa, Phys. Rev. Lett. **93**, 236801 (2004).
[26] J. Homoth, M. Wenderoth, T. Druga, L. Winking, R. G. Ulbrich, C. A. Bobisch, B. Weyers, A. Bannani, E. Zubkov, A. M. Bernhart, M. R. Kaspers, and R. Moöller, Nano Lett. **9**, 1588 (2009).
[27] J. P. Rönspies, S. Wießell, and H. Pfnür, Appl. Phys. A **100**, 1007 (2010).
[28] W. Kern, J. Electrochem. Soc. **137**, 1887 (1990).
[29] A. A. Stekolnikov, K. Seino, F. Bechstedt, S. Wippermann, W. G. Schmidt, A. Calzolari, and M. Buongiorno Nardelli, Phys. Rev. Lett. **98**, 026105 (2007).
[30] U. Gerstmann, N. J. Vollmers, A. Lücke, M. Babilon, and W. G. Schmidt, Phys. Rev. B **89**, 165431 (2014).

[31] S. Chandola, K. Hinrichs, M. Gensch, N. Esser, S. Wippermann, W. G. Schmidt, F. Bechstedt, K. Fleischer, and J. F. McGilp, Phys. Rev. Lett. **102**, 226805 (2009).
[32] H. J. Choi and J. Ihm, Phys. Rev. B **59**, 2267 (1999).
[33] A. Smogunov, A. Dal Corso, and E. Tosatti, Phys. Rev. B **70**, 045417 (2004).
[34] G. Sclauzero, A. Dal Corso, and A. Smogunov, Phys. Rev. B **85**, 165411 (2012).
[35] P. Giannozzi, S. Baroni, N. Bonini, M. Calandra, R. Car, C. Cavazzoni, D. Ceresoli, G. L. Chiarotti, M. Cococcioni, T. Dabo *et al.*, J. Phys.: Condens. Matter **21**, 395502 (2009).
[36] H. J. Monkhorst and J. D. Pack, Phys. Rev. B **13**, 5188 (1976).
[37] D. Karashanova, J. J. Métois, F. Leroy, and P. Müller, Mater. Sci. Sem. Pro. **12**, 12 (2009).
[38] M. Liehr, M. Renier, R. A. Wachnik, and G. S. Sciila, J. Appl. Phys. **61**, 4619 (1987).
[39] T. Hirahara, I. Matsuda, C. Liu, R. Hobara, S. Yoshimoto, and S. Hasegawa, Phys. Rev. B **73**, 235332 (2006).
[40] S. Wippermann, N. Koch, and W. G. Schmidt, Phys. Rev. Lett. **100**, 106802 (2008).